PHYSICAL REVIEW B VOLUME 21, NUMBER 4 15 FEBRUARY 1980

Electronic structure of SiO_2: α-quartz and the influence of local disorder

Roger N. Nucho and Anupam Madhukar
Departments of Physics and Materials Science, University of Southern California, Los Angeles, California 90007
(Received 5 July 1979)

We present a comprehensive study of the electronic structure of α-quartz employing the tight-binding method. Nearest- and second-nearest-neighbor interactions are included and treated as parameters which are adjusted to provide the closest correspondence to the recent pseudopotential-based electronic-structure calculations. A satisfactory agreement over the entire range of bands is obtained employing only eight parameters. Detailed agreement in limited ranges of energies of particular interest in various contexts can be obtained at the cost of discrepancies elsewhere. The direct or indirect nature of the fundamental band gap is found to be controlled by the second-order effects arising from the interplay between the oxygen-oxygen and oxygen-silicon-oxygen interactions. Results for the density of states are obtained and, after proper weighting by the appropriate photoelectric cross sections, compared with the observed x-ray photoelectron spectra (XPS). The computed charge density indicates a charge transfer to oxygen of order unity. The flexibility of the tight-binding method and the insulating nature of SiO_2 are exploited to study the influence of local geometrical distortions from the α-quartz configuration. We find the behavior of the bands near the fundamental band gap to be more sensitive to the precise local geometry than is the overall behavior of the bands. Results for the changes in the bands, density of states, and charge transfer to oxygen as a function of variations in the Si-O-Si bridging-bond angle, as well as the O-O bond length, are presented. It is suggested that such information may be of considerable use in elucidating the nature of amorphous SiO_2. To this end, a framework capable of providing much needed chemical and structural information regarding glassy materials is presented and discussed in the context of recent XPS studies of the core level chemical shifts and of the valence-band structure of amorphous SiO_2.

I. INTRODUCTION

The tight-binding method has proven to be one of considerable flexibility and particular usefulness in studying the electronic structure of complicated lattices of low symmetry. In this paper we exploit this method and present[1] a comprehensive study of the electronic structure of α-quartz, as well as the influence of local disorder. The paper aims at elucidating the influence of different silicon and oxygen interactions (s-s, s-p, and p-p) on the band structure of α-quartz, as well as the role of the Si-O-Si bridging-bond angle and the O-O bond length. This information, it is argued, provides reasonable insights into the behavior of amorphous SiO_2, and possibly even the nature and characteristics of the interface between silicon and its oxide.

To date, theoretical studies of the electronic structure of SiO_2 have employed empirical or semiempirical molecular orbital schemes,[2-5] molecular cluster calculations,[6-10] or phenomenological tight-binding studies of idealized forms of SiO_2 such as β-cristobalite.[11-13] An appraisal of these calculations has been presented by Chelikowsky and Schluter[14] who have recently presented the first study of α-quartz based on the pseudopotential theory. A comprehensive tight-binding study of α-quartz, and particularly the influence of local deformations, is still lacking. It is the aim of the present paper to fill this need. The last section of the paper provides a summary of our findings and places them in proper context in light of recent work.

In Sec. II we develop the basic tight-binding framework and introduce the different types of interactions, namely, nearest- and second-nearest-neighbor matrix elements, as well as the relevant diagonal energies for silicon and oxygen. A procedure for estimating numerical values of some of these parameters is also presented. In Sec. III we present our results for the band structure, the density of states (DOS) and the charge density of α-quartz. We compare the calculated DOS with experimental data obtained via x-ray photoemission spectroscopy[15,16] for the valence bands, after correcting for photoelectric cross-section effects. Section IV is devoted to the study of the effect of local deformation on the electronic structure. In particular we investigate the effects of changing the Si-O-Si bridging-bond angle and the O-O bond length on such properties as the DOS and the charge transfer. Such a study allows reasonable insight and inferences regarding the nature of amorphous SiO_2, which undoubtedly contains a distribution of bond angles and ring sizes of SiO_4 tetrahedral units. In Sec. V we carry these ideas a step further and present a framework in which the distribution of silicon to oxygen charge transfer, corresponding to a distribution of the bridging oxygen bond angle, is suggested to give rise to a distribution of core-level chemical shifts. It is argued that if this dis-

tribution is peaked at certain bond angles, then the corresponding core-level shifts could become observable in high resolution XPS studies. Recent work of Grunthaner *et al.*[16] gives credence to these ideas. In Sec. VI we conclude with a discussion and some comments on future directions of the present studies.

II. TIGHT-BINDING MODEL

A. Structure and basis functions

The primitive cell of α-quartz is hexagonal, containing three Si atoms and six oxygen atoms, as shown in Fig. 1(a) along with the set of Cartesian coordinates employed in this study. The corresponding Brillouin zone[17] is drawn in Fig. 1(b). Note the four equivalent Si atoms at four edges of the primitive cell and the two equivalent atoms at two of the faces.[18] The tight-binding basis functions are written in the conventional manner as

$$\psi_{\nu,\beta}(\vec{k},\vec{r}) = \frac{1}{\sqrt{N}} \sum_l e^{\vec{k}\cdot\vec{R}_l} \psi_\nu(\vec{r} - \vec{R}_l - \vec{\tau}_\beta) , \qquad (1)$$

where l is a sum over the N lattice points, $\beta = 1, \ldots, 9$ locates the particular type of atom considered within the primitive cell, and ν denotes the type of atomic orbital. The Si $3s$ and $3p$ atomic levels lie at -13.55 and -6.52 eV, respectively, while the O $2s$ and $2p$ levels lie at -29.14 and -14.13 eV, respectively. The O $2s$ level lying much lower than the other levels considered, is not expected to mix much with these orbitals. Evidence for this weak mixing has also been found in previous studies.[8,11,14] While retaining the O $2s$ orbital does not add any significant difficulty in the analysis, it is nevertheless omitted from our basis set. We are thus left with 30 functions: the four sp^3 hybrids around each of the three Si atoms and three p orbitals (p_x, p_y, p_z) for each of the six oxygens. These functions yield 30 bands, only 18 of which are filled by the 36 valence electrons per cell (four on each Si and four on each O). Note that inclusion of oxygen $2s$ levels would result in 36 bands, 24 of which would be filled since there would be, in that case, 48 valence electrons per cell (four on each Si and six on each O). Ignoring the O $2s$ levels, then, amounts to omitting a lower-lying manifold of six valence bands of essentially O $2s$ character.

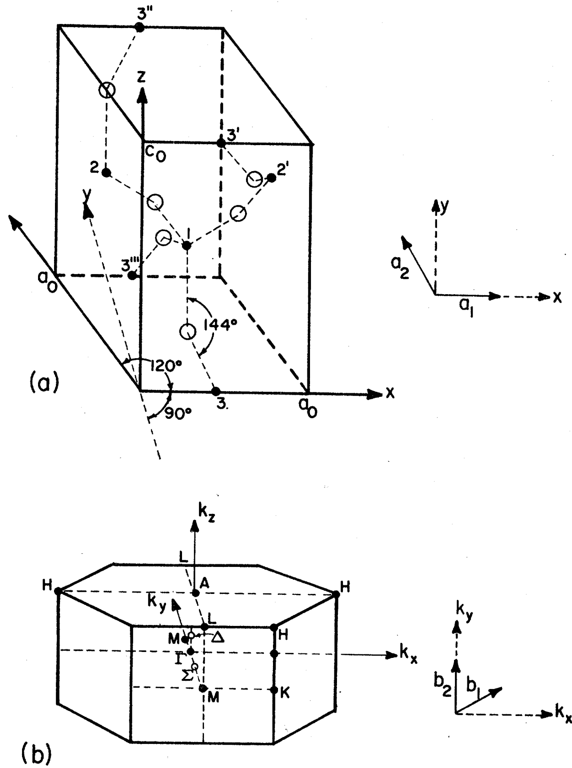

FIG. 1. (a) Primitive cell for α-quartz. Atoms labeled by the same number are equivalent. a_1 and a_2 are the primitive translation vectors in the x-y plane. (b) Corresponding Brillouin zone. b_1 and b_2 are the reciprocal lattice translation vectors in the k_x-k_y plane.

B. Nearest-neighbor interactions

In setting up the calculations it was found profitable to view the system as alternating Si-O-Si and O-Si-O triads (see Fig. 2). Each Si-O-Si triad determined three directions ϵ_σ, $\epsilon_{\pi 1}$, and $\epsilon_{\pi 2}$ which we shall refer to as the triad coordinate system. ϵ_σ is parallel to the Si-Si directions, $\epsilon_{\pi 1}$ is perpendicular to ϵ_σ but lies in the plane of the triad, and $\epsilon_{\pi 2}$ is normal to that plane. The three oxygen p orbitals were taken along these directions and will, consequently, be denoted by p_σ, $p_{\pi 1}$, and $p_{\pi 2}$. The Si basis functions were taken to be the sp^3 hybrids as mentioned above, but the hybrids were then expanded in terms of the Si s and p orbitals in the triad coordinate system so that the nearest-neighbor matrix elements of the Hamiltonian could ultimately be described in terms of s and p functions, as shown in Fig. 2. We have shown six nearest-neighbor (n.n.) parameters. These interactions may be assumed to be independent, giving rise to a tight-binding description involving six adjustable n.n. parameters. However, invoking certain geometric relationships along with the commonly employed two-center approximation, one can easily show that these six n.n. interaction parameters are related, thus leading to only three independent parameters. These three parameters are taken to correspond to linear Si-O-Si bonds. The expressions relating the six n.n. matrix elements to the fundamental three, which we denote as $V^0_{sp\sigma}$, $V^0_{pp\sigma}$, and $V^0_{pp\pi}$, are

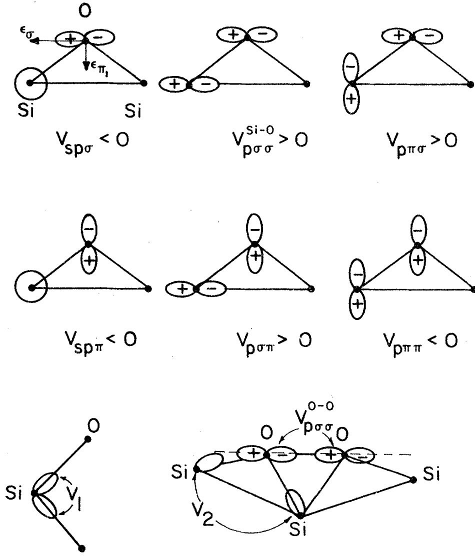

FIG. 2. Nearest-neighbor and second-nearest-neighbor interactions considered (except V_1 which is an on-site parameter).

$$\begin{aligned} V_{sp\sigma} &= \cos\alpha\, V_{sp\sigma}^0\,, \\ V_{sp\pi} &= \sin\alpha\, V_{sp\sigma}^0\,, \\ V_{p\sigma\sigma}^{\mathrm{Si-O}} &= \cos^2\alpha\, V_{p\sigma\sigma}^0 + \sin^2\alpha\, V_{p\pi\pi}^0\,, \\ V_{p\pi\pi} &= \sin^2\alpha\, V_{p\sigma\sigma}^0 + \cos^2\alpha\, V_{p\pi\pi}^0\,, \\ V_{p\pi\sigma} &= V_{p\sigma\pi} = \sin\alpha\, \cos\alpha\,(V_{p\sigma\sigma}^0 - V_{p\pi\pi}^0)\,, \end{aligned} \tag{2}$$

where α is the O-Si-Si angle in the Si-O-Si triad (see Fig. 2) and is equal to 18° for α-quartz. The three fundamental n.n. parameters thus correspond to $\alpha=0$ and may be visualized by setting $\alpha=0$ in Fig. 2.

C. Other interactions

The second-neighbor interactions are of two types: Si-Si and O-O. Of the Si-Si interactions, we retain only the interaction between hybrids belonging to the given Si-O-Si triad, denoted by V_2 in Fig. 2. The O-O interactions require a somewhat more involved analysis. Each of the oxygen p_σ, $p_{\pi 1}$, and $p_{\pi 2}$ orbitals is expanded along the appropriate O-O direction, yielding a component parallel to that direction and proportional to $V_{p\sigma\sigma}$ as well as a component normal to that direction which we will neglect. Earlier estimates[12] have shown that this normal component is less than 10% of the parallel component. The remaining matrix elements of the problem are three diagonal energies, $E(sp^3)$, $E(p_{ox})$ and V_1, where $E(sp^3)$ is the silicon hybrid energy, $E(p_{ox})$ is the oxygen $2p$ energy, and $V_1=(\epsilon_S^{Si}-\epsilon_p^{Si})/4$. The total number of parameters is thus eight (three diagonal energies, three n.n. interactions, and two second-neighbor interactions), if we invoke the true two-center approximation,[19] or eleven, if one chooses to consider all six n.n. interactions as independent parameters, as noted previously. Results for both these situations are presented in Sec. III.

D. Density of states

The expression for the density of states (DOS) is

$$N(E)=\sum_{n,k}\delta(E-E_n(k))\,.$$

The δ function appearing in the above expression was approximated by a Gaussian of width σ. Thus the DOS, normalized to one, was obtained by computing

$$N(E)=\frac{1}{60N}\sum_{n,k}\frac{1}{\sigma(2\pi)^{1/2}}\exp\left(-\frac{[E-E_n(k)]^2}{2\sigma^2}\right). \tag{3}$$

Various widths were taken for σ, and the results for $\sigma=0.5$ eV are given in this paper. Grids containing 75 and 196 mesh points in the irreducible part of the Brillouin zone were used. The 75-point grid was found to be satisfactory.

E. Charge density

Within the tight-binding framework, the total charge density is easy to evaluate. Writing the eigenfunction for band n as

$$\Phi_n(\vec{k},\vec{r})=\sum_\lambda\sum_\beta C_{\lambda\beta}^n(\vec{k})\Psi_{\lambda,\beta}(\vec{k},\vec{r})\,, \tag{4}$$

the total charge density about the Si atom, for instance, is given by

$$Q_{\mathrm{Si}}=2\sum_v\sum_k\sum_{\lambda\beta}{}' C_{\lambda\beta}^{v*}(k)C_{\lambda\beta}^v(k)\,, \tag{5}$$

where v stands for valence band, the factor 2 arises from the sum over spin, and the prime on the last sum restricts it to Si atoms. The sum over k space was evaluated using the Baldareschi scheme generalized by Chadi and Cohen[20] to hexagonal lattices. We used, successively, 3, 6, and 12 special points, and found the convergence to be very good even with three points alone.

F. Estimation of parameters

To initiate the calculations, a set of parameters was estimated via a combination of previously quoted values in the literature and certain empirical chemical rules which have come to be of great value in estimation of bond strengths. Thus, for example, an initial estimate of the $V_{p\sigma\sigma}^{\mathrm{Si-O}}$ matrix element of the interaction between silicon and oxygen was obtained by taking the geometric mean of the corresponding Si-Si and oxygen-oxygen matrix elements, scaled to the appropriate Si-oxygen dis-

tance of 1.61 Å for α-quartz. The geometric mean is taken in the spirit of the Pauling geometric mean rule for bond energies and is considered to be a good starting point, even though one recognizes that the matrix elements are not the same as bond energies, as well as the fact that correction for the partly ionic nature of the Si-O bond should also be accounted for. The scaling with respect to changes of the bond lengths was done following the "inverse square" behavior of the tight-binding parameters found by Harrison. In particular, the work[12] of Pantelides and Harrison on β-cristobalite estimates $V_{p\sigma\sigma}^{O-O}$ to be 1.45 eV and $V_{p\pi\pi}^{O-O} \simeq -0.17$ eV (i.e., 12% of $V_{p\sigma\sigma}^{O-O}$) for oxygen atoms separated by 2.60 Å. A tight-binding study[21] of silicon by Pandey and Phillips gives the value $V_{p\sigma\sigma}^{Si-Si} = 2.32$ eV for silicon atoms separated by 2.35 Å. Scaling these numbers to the distance 1.61 Å gives $V_{p\sigma\sigma}^{O-O} = 3.78$ eV and $V_{p\sigma\sigma}^{Si-Si} = 4.94$ eV, whence the geometric mean rule gives $V_{p\sigma\sigma}^{Si-O} = 4.32$ eV. In a similar manner, from the value of $V_{p\pi\pi}^{Si-Si}$ in Si (−0.52 eV) (Ref. 21) and $V_{p\pi\pi}^{O-O}$ in SiO_2 (−0.17 eV),[12] the value of $V_{p\pi\pi}^{Si-O}$ was estimated to be −0.70 eV.

In addition, from the work[12] of Pantelides and Harrison, estimates can be obtained for the two parameters W_{2x} and W_{2z} describing the matrix elements of the Hamiltonian between a Si sp^3 hybrid and the oxygen $p_{\pi 1}$ and p_σ orbitals, respectively. Using simple geometry, W_{2x} and W_{2z} may be expanded in terms of the parameters of this analysis, obtaining

$$W_{2x} = -\langle \psi_{sp^3} | H | p_{\pi 1} \rangle = -\tfrac{1}{2}(V_{sp\pi} - \sqrt{3}\cos 18^\circ\, V_{p\sigma\pi} - \sqrt{3}\sin 18^\circ\, V_{p\pi\pi}),$$

and (6)

$$W_{2z} = -\langle \psi_{sp^3} | H | p_\sigma \rangle = -\tfrac{1}{2}(V_{sp\sigma} - \sqrt{3}\cos 18^\circ\, V_{p\sigma\sigma}^{Si-O} - \sqrt{3}\sin 18^\circ\, V_{p\pi\sigma}).$$

Values for W_{2x} and W_{2z} may be obtained from Eqs. (2) of Ref. 12 using the given value of 10.75 eV for W_2. The overlap S was taken to be zero. Bearing in mind that $V_{sp\pi} = V_{sp\sigma}^0 \sin 18^\circ$, $V_{sp\sigma} = V_{sp\sigma}^0 \cos 18^\circ$, and that $V_{p\sigma\pi} = V_{p\pi\sigma}$, and given the estimates for W_{2x} (2.32), W_{2z} (10.22), $V_{p\sigma\sigma}^{Si-O}$ (4.32), and $V_{p\pi\pi}$ (−0.70), one can obtain from Eqs. (6) values for $V_{sp\pi}$ (−3.97), $V_{sp\sigma}$ (−12.22), and $V_{p\pi\sigma}$ (1.2). However, noting that the $V_{p\sigma\sigma}$ overlap is expected to be larger than the $V_{sp\sigma}$ overlap, the value of $V_{p\sigma\sigma}$ was increased until the value of $|V_{sp\sigma}|$ determined via Eqs. (6) became smaller than $V_{p\sigma\sigma}$. The Si-Si interaction was estimated by similar considerations, and the diagonal parameters were taken to be the atomic term values. The starting set of parameters was then estimated to be the following (all energies are in eV): $E(sp^3) = -8.28$, $E(p_{ox}) = -13.14$, $V_1 = -1.76$, $V_{sp\sigma} = 6.32$, $V_{sp\pi} = -2.07$, $V_{p\sigma\sigma}^{Si-O} = 7.50$, $V_{p\sigma\pi} = V_{p\pi\sigma} = 3.00$, $V_{p\pi\pi} = -0.70$, $V_2 = -2.30$, and $V_{p\sigma\sigma}^{O-O} = 1.45$ eV. Note that the values given above are also consistent with relations (2). Starting from this set, the parameters were adjusted to obtain the best fit to the bands provided by the recent pseudopotential calculations.[14] It is in this fitting procedure that the tight-binding method provides much needed insight into the particular influence of the various interaction parameters on the band structure. A rather comprehensive study of such effects, including different fits corresponding to different criterion (motivated by particular questions of relevance in different context), results for the density of states, and the charge transfer from silicon to oxygen for α-quartz is the subject of the next section. In Sec. IV we examine the influence of the departure from the α-quartz geometry.

III. RESULTS FOR α-QUARTZ

A. Band structure

Experience with the tight-binding calculations in various contexts has established that, while satisfactory fits to limited energy and momentum regions of the band structure of the system of interest may be achieved with a reasonable number of tight-binding parameters, an accurate fit over the entire Brillouin zone for many bands is generally not possible without an unduly large number of parameters. This is particularly true of complicated lattice structures of low symmetry involving large unit cells. To maintain the smallest possible number of parameters, as well as keeping in mind the future use of these parameters in investigating the influence of geometrical distortions, it was found profitable to consider two types of fits. One is the best overall fit for all the bands covering an energy range of the order of 40 eV for SiO_2. The other is the best fit to the valence bands, obtained at the cost of a less accurate description of the conduction bands. Furthermore, for each of these two cases we provide two sets of parameters: one corresponding to eight parameters only while the other corresponds to 11 parameters. We recall from Sec. II that, while the latter case treats all nearest-neighbor interactions as distinct and independent parameters, the former makes use of Eqs. (2) resulting from geometrical relationships implied by the two-center approximations. In the following, therefore, we will refer to these as the eight-parameter or 11-parameter fit with the above understanding of the difference between them.

In Table I, the various sets of parameters are given. Set 1 constitutes the best overall fit achieved with 11 parameters. The corresponding band structure for two directions in the Brillouin zone is shown in Fig. 3. Set 2 gives the best overall fit

TABLE I. Tight-binding parameters for α-quartz. Set 1 corresponds to the 11-parameter overall fit, set 2 to the eight-parameter overall fit, set 3 to the 11-parameter valence-band fit, and set 4 to the eight-parameter valence-band fit. Absolute values of the diagonal parameters are chosen such that the topmost valence band at Γ point is at zero energy. All parameters are in eV.

	$E(sp^3)$	$E(p_{ox})$	V_1	$V_{sp\sigma}$	$V_{p\sigma\sigma}^{\text{Si-O}}$	$V_{p\sigma\pi}$	$V_{pp\sigma}$	$V_{sp\pi}$	$V_{p\pi\pi}$	V_2	$V_{p\sigma\sigma}^{\text{O-O}}$
Set 1	−12.54	−1.30	1.6	−7.00	9.00	4.00	4.00	−0.80	−0.70	1.50	1.76
Set 3	−10.32	−1.94	−1.10	−5.00	5.50	3.00	3.00	−0.80	−0.70	1.50	1.55

	$E(sp^3)$	$E(p_{ox})$	V_1	$V_{sp\sigma}^0$	$V_{p\sigma\sigma}^{0\text{Si-O}}$	$V_{p\pi\pi}$	V_2	$V_{p\sigma\sigma}^{\text{O-O}}$
Set 2	−10.55	−0.70	−2.00	−7.00	10.15	−1.84	1.50	1.00
Set 4	−8.98	−1.28	−1.10	−4.70	6.23	−1.43	1.50	1.20

employing only eight parameters, the corresponding bands being shown in Fig. 4(a). Although we have not superimposed on either Figs. 3 or 4 the band structure obtained from the pseudopotential calculations, nevertheless, examination shows that the bands of Fig. 4(a) are slightly less accurate, as is expected, owing to the reduced number of parameters. Set 3 corresponds to the best 11-parameter fit to the valence-band region alone [Fig. 4(b)], while set 4 yields the best eight-parameter fit to that same region [Fig. 4(c)]. Table II provides a comparison between eigenvalues obtained within the eight-parameter fits (sets 2 and 4) and the pseudopotential calculations.

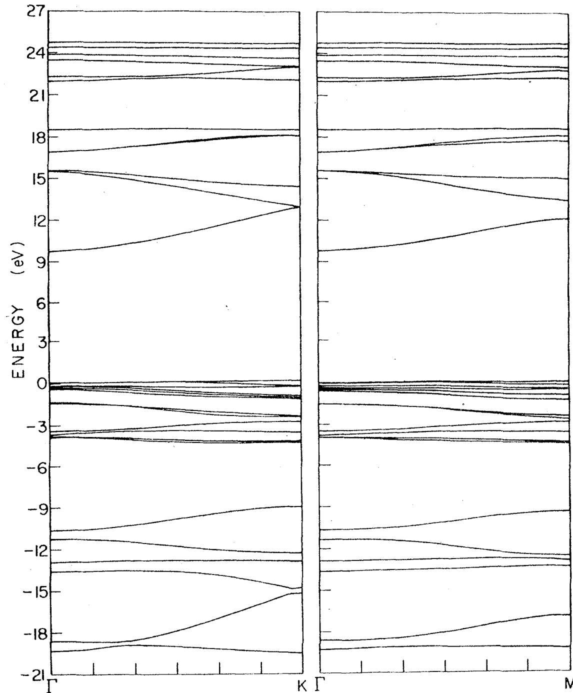

FIG. 3. Energy bands for α-quartz along the K and M directions corresponding to set 1 of the parameters.

Next, we discuss the individual effect of each of the parameters shown in Fig. 2. The oxygen $p_{\pi 2}$ orbital, normal to the Si-O-Si plane, does not interact strongly with the Si orbitals. Thus, the topmost valence bands which are largely derived from these oxygen orbitals have been referred to as "nonbonding." However, all the oxygen p orbitals (including the $p_{\pi 2}$ orbital) interact with the second-nearest-neighbor oxygen p orbitals. Each of these interactions may be written as the sum of two terms, one proportional to $V_{p\sigma\sigma}^{\text{O-O}}$ (i.e., along the O-O direction), and one proportional to $V_{p\pi\pi}^{\text{O-O}}$ (i.e., one perpendicular to the O-O direction). In our analysis, the $V_{p\pi\pi}^{\text{O-O}}$ component is neglected, hence it is the parameter $V_{p\sigma\sigma}^{\text{O-O}}$ which directly controls the width of these nonbonding bands (bands 7 through 18, counting from the bottom of the figures). The lower valence bands (1 through 6) and the upper conduction bands (25 through 30) arise from the strong nearest-neighbor interactions between the Si atom and the oxygen p_σ orbital. Con-

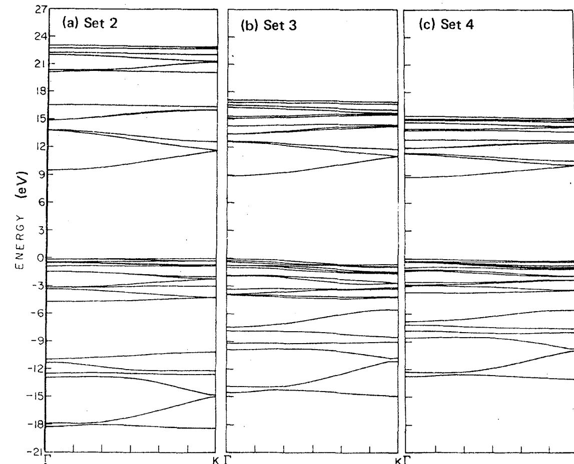

FIG. 4. Energy bands for α-quartz along the K direction corresponding to (a) set 2, (b) set 3, and (c) set 4 of the parameters.

TABLE II. Shows a comparison between eigenvalues at certain high symmetry points obtained within the eight-parameter fit and pseudopotential calculations. Note that labeling of the bands is in ascending order (1 through 30), band 18 being the topmost valence band. All values are in eV.

	Set 2	Set 4	Pseudopotential
Γ_7	−4.58	−3.6	−4.2
Γ_{18}	0.0	0.0	0.0
Γ_{19}	9.59	8.82	9.7
K_7	−4.2	−3.5	−4.4
K_{18}	0.08	−0.19	0.5
K_{19}	11.7	10.18	14.5
M_7	−4.2	−3.4	−4.4
M_{18}	0.06	−0.21	−0.13
M_{19}	11.14	9.82	12.53

sequently, the widths of these bands is basically controlled by $V_{sp\sigma}$ and $V_{p\sigma\sigma}^{Si-O}$. The lowest conduction band at the Γ point is of pure Si-s symmetry, whereas it has some oxygen p_σ mixing everywhere else. Thus the parameter $V_{sp\pi}$ acts like a "fine tune" for the gap at the Γ point. The magnitude of the fundamental band gap is controlled mainly by the diagonal energies, and the atomic term values were found to give much too small a gap compared to the generally accepted value of ~9.00 eV. It was necessary to force a large separation between the Si and oxygen diagonal energies. Furthermore, it is of interest to note that the indirect gap was found to arise from a second-order effect involving the O-Si interaction, $V_{p\sigma\sigma}^{Si-O}$. It is only when this parameter is made large in the presence of a nonzero $V_{p\sigma\sigma}^{O-O}$ that an indirect gap is obtained. In the process, however, there results an excessive lowering of the lower-lying valence bands. Thus, the basic difference between the "overall" fits (sets 1 and 2) and the "valence region" fits (sets 3 and 4) is that in the former an indirect gap is obtained, but along with a set of six valence bands lying as deep as −20 eV (with respect to the top of the valence bands), whereas in the latter the lowest valence band lies closer to the experimental value of about −12.5 eV, but the indirect nature of the gap is lost. As for the parameters $V_{p\sigma\pi}$ and $V_{p\pi\sigma}$, their main effect is to control the width of the lower-lying valence bands, more specifically the separation between bands 2 and 3. Finally, the parameters $V_{p\pi\pi}$ and V_2 were found to have relatively minor effects. $V_{p\pi\pi}$ affects the overall dispersion somewhat, and V_2 displaces the lowest conduction band a little.

It must be noted that the final value for V_2 resulting from the fits is 1.5 eV as opposed to the estimated value of −2.3 eV. This difference in sign of V_2 is the only significant departure of the final parameters from their initial estimated values and requires comment. It has been noted[19] by Slater and Koster that the second-nearest-neighbor interactions in a tight-binding study, when treated as parameters, may turn out to have the opposite sign to that one may *a priori* have expected. We refer the reader to the original discussion of this point given by these authors, but merely note that such changes in the sign of second-nearest-neighbor parameters are found to be a rather common feature of tight-binding fits. Nevertheless, to obtain a better insight into the role of the parameter V_2, two checks were made. First, an examination of an isolated Si-O-Si triad obtained by turning off all interactions between the various triads shows that the total electronic energy of the triad is lower with V_2 positive rather than negative. Second, a positive sign for V_2 increases the value of the fundamental gap by raising the lowest conduction band. This allows for a smaller separation between the silicon and oxygen diagonal energies required to produce the experimental band gap. Since the charge transfer from silicon to oxygen is directly coupled to the separation of the diagonal energies, we find that a smaller separation gives rise to charge transfer more in keeping with the expected ionicity of the silicon-oxygen band. Both these features strongly argue in favor of a positive sign for V_2, at least in a parametrized study.

B. Density of states and x-ray spectrum

In Fig. 5 is shown the density of states for set 2 of the parameters. The gap between the upper (nonbonding) set of valence bands and the lower (bonding) set is largely due to the parameter $V_{p\sigma\sigma}^{Si-O}$. The large peak at the valence band edge is caused by the lack of dispersion in the uppermost nonbonding bands (0 to −2 eV), a feature present in the pseudopotential calculations (note peak A in Fig. 2, Ref. 14). In Figs. 6(a), 6(b), and 6(c) are

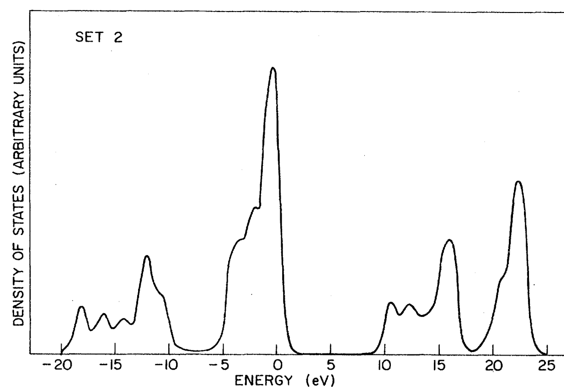

FIG. 5. Density of states for α-quartz corresponding to set 2 of the parameters.

shown, respectively, the s contribution to the DOS, the p contribution, and the total DOS for set 4 of the parameters. (Recall that this set consists of eight parameters only.) Only the valence-band region is shown. It can be seen that the s contribution to the valence bands is small [Fig. 6(a)] and that the valence band edge is mainly of p character [Fig. 6(b)].

A comparison with x-ray photoelectron spectra (XPS) requires an appropriate weighting of the s and p DOS by the corresponding photoelectric cross sections. Thus Fig. 6(d) represents the valence band DOS weighted by s and p photoelectric cross sections at 1487 eV taken from theoretical calculations by Scofield[22] for Si and O *atoms*. The ratio of the s to p cross sections is about 10. In Fig. 7 is shown a similar plot (curve a) with an s to p cross-section ratio of about 20, for comparison with XPS for α-quartz[15] (curve b) and a-SiO_2 (Ref. 16) (curve c). Note the vertical displacement of the three curves for clarity. The zero of energy indicates the true valence band edge. The tailing of the density of states up to about +1 eV beyond is a

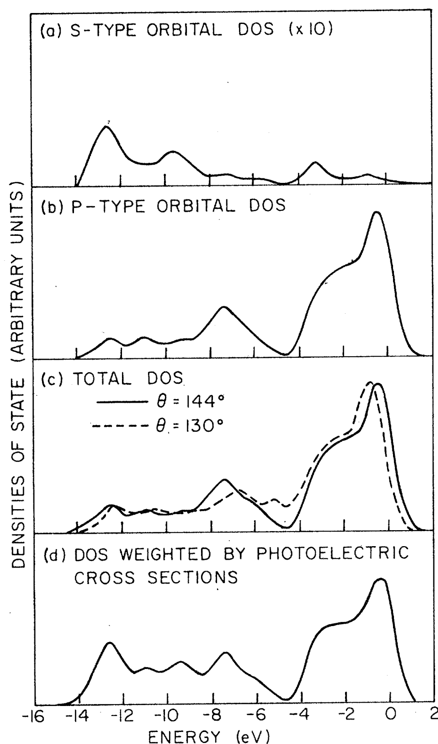

FIG. 6. Densities of state for α-quartz corresponding to set of 4 of the parameters. (a) s-type orbital DOS, (b) p-type orbital DOS, (c) total DOS for α-quartz (solid line) and for a deformation of the Si-O-Si angle by 14° (dotted line), and (d) total DOS weighted by the s and p photoelectric cross sections given in Ref. 22 (ratio of s to p cross sections is approximately ten).

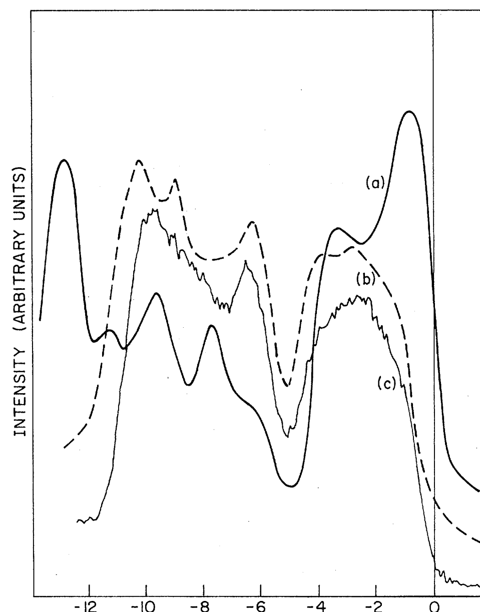

FIG. 7. Photoelectric cross-section weighted density of states with an s to p cross-section ratio of about 20 (curve a), XPS for α-quartz (curve b), and a-SiO_2 (curve c).

consequence of the Gaussian width employed for computational ease. The agreement with experiment may be improved by a different choice of parameters corresponding to a different band fit.

C. Charge transfer

Following the procedure outlined in Sec. II the charge transfer from Si to oxygen was calculated for the α-quartz geometry. The charge transfer per Si-O bond is found to be 0.58, 0.51, 0.65, and 0.61 for sets 1, 2, 3, and 4, respectively, in units of electronic charge. As noted before, the magnitude of this charge transfer depends largely on the difference between the two diagonal energies, $E(\mathrm{ox}) - E(sp^3)$.

IV. INFLUENCE OF LOCAL DISTORTIONS

In this section the flexibility of the tight-binding method is exploited to investigate the effect of various deformations of the SiO_2 unit cell on the electronic structure. Referring to Fig. 2, it can be seen that since the interactions are explicitly described by overlapping orbitals, any change in the triad configuration from the α-quartz geometry will lead to a change in the matrix elements which can be calculated by simple geometry from the values obtained for α-quartz in the preceding section.

These studies of the influence of variations in the Si-O-Si bridging-bond angle and the oxygen-

oxygen distance are motivated by the well documented evidence[23] for such variations in amorphous SiO_2 and glassy materials in general. The insulating nature of SiO_2 lends support, of course, for the relevance of tight-binding studies, but also supports the "local chemical environment" point of view behind our use of this method for studying the influence of local geometrical distortion. Inherent in this point of view is the idea that the basic electronic nature of the material is determined, for all practical purposes, essentially by the geometry and chemical interactions of nearest and second-nearest neighbors. Thus the distortions introduced within the unit cell of α-quartz should be a reasonable starting point for investigations of the influence of short-range disorder. The use of the tight-binding method may then be considered as a simple way of imposing periodic boundary conditions for calculational purposes, on a "molecular cluster" which is considered to be the unit cell. In principle, of course, one may consider clusters larger than the three silicons and six oxygens of α-quartz when deformations are introduced. Indeed, one may argue that a decrease, for example, of the bridging Si-O-Si bond angle at one place would have to be somehow compensated for by an increase nearby, so as to keep the strains inside the solid to a minimum. This would, of course, require an enlargement of the size of the unit cell.

It may, however, be argued that, to the extent that the chemical nature of the solid may be governed primarily by the nearest- and second-nearest-neighbor interactions, the main features of the electronic structure of the solid would be quite well reflected in the combination of results of the present "nine atom cluster" unit cell calculations for deviations towards smaller and larger bridging-bond angles.

A. Si-O-Si bond angle changes

To first order, the second-nearest-neighbor parameters are unchanged, while the new "effective" nearest-neighbor parameters may be evaluated via Eqs. (2), as a function of the bridging oxygen bond angle. In Fig. 6(c) the total DOS for a Si-O-Si angle of 130° (dotted line) is shown for comparison with the α-quartz case (solid line). Note the appearance of states in the "gap" between the nonbonding and bonding valence bands. This filling of the gap is due to a decrease in the parameter V_p^{Si-O}, as pointed out before. Note also the displacement of the nonbonding valence bands to lower energy. The conduction band edge (not shown) moves to higher energy, thereby increasing the fundamental gap. The displacement of the nonbonding valence bands is essentially due to the decrease in V_p^{Si-O}, while the change in the conduction band edge is due to the increase in the magnitude of the parameter $V_{sp\pi}$. The opposite effects are found when the Si-O-Si angle is made larger than the α-quartz value of 144°.

The changes in the value of the charge transfer as a function of the Si-O-Si angle were also studied. The results are plotted in Fig. 8 for the four sets of parameters. The four curves are essentially similar in shape but translated vertically with respect to each other. It can thus be seen that for either the overall fits (sets 1 and 2) or for the valence-band fits (sets 3 and 4), the absolute magnitude of the charge depends mainly on the difference between $E(\text{ox})$ and $E(\text{Si } sp^3)$, whereas the relative variation (as a function of angle) is almost independent of this difference.

B. Variation in O-O separation

A study of the influence of variation in the oxygen-oxygen separation is of value in isolating and understanding the basic interactions which control the behavior of the topmost nonbonding valence bands. Two basic approaches to modeling the changes in the oxygen-oxygen separation may be followed. One is to allow the O-Si-O angle to change without letting the $Si(sp^3)$ hybrids follow the Si-O bond direction. The other is to keep the hybrids pointing in the bond direction, thereby changing the tetrahedral angles between the hybrids. Some specific considerations required by the latter

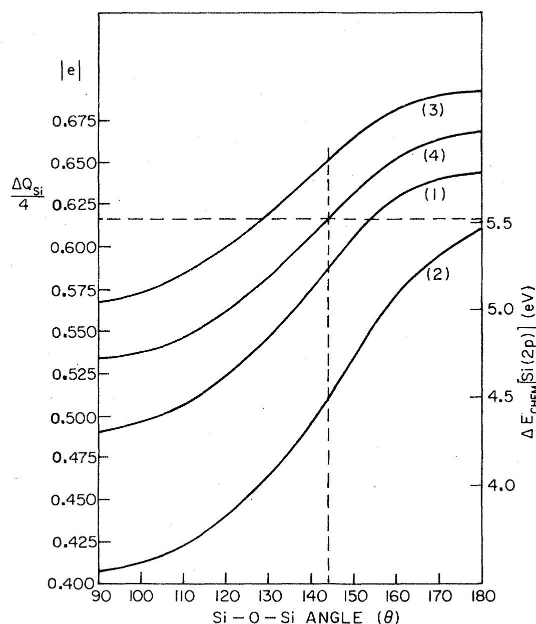

FIG. 8. Silicon to oxygen charge transfer (per Si–O bond) as a function of the bridging oxygen bond angle θ. Curves 1 through 4 correspond to the sets of parameters 1 through 4. The Si (2*p*) chemical shift shown corresponds to curve 2.

situation will be taken up elsewhere.[24] However, we have noted earlier[1] that, even when the tetrahedral angle is allowed to change, it is the attendant change in oxygen-oxygen interaction ($V_{p\sigma\sigma}^{O-O}$) which influences the electronic structure the most. This, combined with the fact that the tetrahedral angle is harder to change, leads us to follow, for the purposes of the present study, the former approach. The change in the oxygen-oxygen separation is modeled as a change in the oxygen-oxygen interaction parameter $V_{p\sigma\sigma}^{O-O}$ via an inverse-square dependence on the separation. As indicated in the previous section, this parameter is the crucial one in determining the width of the nonbonding valence bands: the larger $V_{p\sigma\sigma}^{O-O}$, the larger the width of the nonbonding bands. The point is well illustrated and confirmed by a consideration of GeO_2. The average O-O separation in GeO_2 is larger than α-quartz, and consequently, the overlap of the oxygen p orbitals is smaller. As a result, $V_{p\sigma\sigma}^{O-O}$ should be smaller and the nonbonding bands of GeO_2 narrower, as they are. It is worth noting here that variations in the Si-O-Si angle do not significantly influence the width of the nonbonding valence bands as can be seen in Fig. 6(c). These observations thus substantiate the speculation[15] by Fischer *et al.* that the dominant parameter determining the nonbonding valence bands of the $Si_xGe_{1-x}O_2$ series is the shortest oxygen-oxygen separation, rather than the Si-O-Si band angle.

V. LOCAL STRUCTURE AND CORE LEVEL CHEMICAL SHIFTS

An essential feature of the ideas investigated in the previous section is the interdependence of the chemical and structural environment on a local or short-range scale. In the present section this central though is taken a step further by presenting arguments which exploit core-level chemical shift information to deduce local structural information in glassy materials. Although these ideas are presented in the context of amorphous SiO_2, their more general validity is self-evident.

Traditionally,[25] the notion of core-level chemical shift has been associated with core-level binding energy changes arising from changes in the valence charge distribution caused by the presence of a chemically different species in the vicinity. However, we exploit the fact that even a change in the local structure can give rise to changes in valence charge distribution, thus inducing core-level chemical shifts. The question at this point naturally takes on a quantitative stance. Whether or not the changes in the valence charge, attendant to the expected range of structural geometries, are sufficient to cause observable chemical shifts in the available core levels is a basic question but one which can be dealt with case by case only. The calculated variations in the silicon to oxygen charge transfer as a function of the bridging oxygen bond angle (Fig. 8) of the preceding section, combined with recent XPS studies[16] of amorphous SiO_2-indicate that such effects may already have been found in this system.

Although the details of the structure of glasses in general and SiO_2 in particular remains an important problem,[26,27] nevertheless a variety of experiments tends to offer considerable evidence that SiO_4 tetrahedron tends to maintain its integrity even in the amorphous phase. These tetrahedra are held together via a bridging oxygen, thus forming a ring structure.[27] It is speculated that the amorphous phase consists of a distribution of ring sizes,[28] possibly ranging from rings consisting of as few as three SiO_4 tetrahedra to as many as eight and possibly higher. This distribution of ring size is made possible, to a large extent, by the flexibility of the Si-O-Si bond angle subtended at the bridging oxygen. It is also likely that for given ring sizes the bridging oxygen bond angle has a distribution although it is *a priori* not clear, of course, how sharply such a distribution may be peaked in the amorphous phase. Some insight into the likely connection between a given ring size and the corresponding most probable bridging oxygen bond angle may be gained by an examination of the reported structural properties of the various polymorphs of SiO_2. We refer the reader to the rather extensive compilation and analysis[29] of such data provided by Hubner in the recent past. However, for ready reference in Table III we have provided some relevant information. It is readily seen that the existing polymorphs of SiO_2 do suggest a strong correlation between ring size and the bridging oxygen bond angle. It is entirely plausible, then, that the silicon to oxygen charge transfer calculated in the previous section as a function of the Si-O-Si bond angle may reflect the influence of ring size as well.

TABLE III. Silicon-oxygen-silicon bridging angle and the corresponding ring structure for various SiO_2 polymorphs.

Material	Si-O-Si angle	Ring size [c]
Coesite	120° [a]	4
α-quartz	144° [a]	6
β-cristobalite	⩾165°	7-8-9
Keatite	154° [b]	5-7-8

[a] Reference 28.
[b] Reference 29.
[c] Reference 27.

The calculations of the preceding section and the above arguments thus suggest that amorphous SiO_2 may very well exhibit different Si(2*p*) and O(1*s*) core-level shifts corresponding to the predominance of certain Si-O-Si bond angles. If observable, such peaks and their line shapes can be powerful tools for studying local geometrical structure. However, purely theoretical estimation of core-level binding-energy shifts corresponding to a given charge transfer, by and large, remains a rather complicated problem, if not a formidable one, also. Consequently, attempts have been made in the past to seek correlations between experimentally observed chemical shifts and such phenomenological concepts as electronegativity. For instance, a compilation of Si(2*p*) binding energies in 33 organosilicon compounds as functions of different electronegativities, given by Pauling, Jolly, Sanderson, and CNDO calculations, may be found in a recent paper[30] by Gray *et al.* For SiO_2 itself, the material of interest to us, Hubner has attempted[29] to formulate an ionicity of the Si-O bond based on Phillip's definition of ionicity in terms of optical properties. He has thus extracted a Si-O ionicity versus the bridging oxygen bond angle curve from the relevent experimental values for various polymorphs of SiO_2. However, the conversion of this ionicity into charge is a procedure whose reliability cannot be easily assessed.[31]

Following this phenomenological approach, we rely upon the experiment for a scale factor which converts the calculated silicon to oxygen charge loss (Fig. 8) into a binding energy shift of the Si(2*p*) core level. Such a scale factor may be obtained by taking the measured separation in the Si(2*p*) core-level binding energies of elemental silicon and silicon in α-quartz, and dividing it by the calculated charge transfer from silicon to oxygen in α-quartz (i.e., for Si-O-Si bond angle of 144°). This scale factor, which gives the Si(2*p*) binding-energy shift per unit charge transfer, may then be used to convert the curves of Fig. 8 into a measured binding-energy shift versus Si-O-Si bond angle realtion. In obtaining a scale factor in this fashion, it is assumed that the final state relaxation effects are not unduly sensitive to local geometry and are roughly the same in the condensed phase.[29] On the other hand, being a phenomenological scale factor, it contains, albeit in an unknown way, the influence of the extra atomic chemical shifts. It is thus expected to be a rather reliable scale factor for obtaining a reasonable idea of expected binding energy shifts in situations where no other means is presently available. The full implications of such an analysis can be best appreciated in conjunction with a detailed and critical experimental study, such as provided by Grunthaner *et al.* elsewhere.[32] Here, for completeness of the notions, we briefly discuss the process of extracting the scale factor.

Recently, Grunthaner and coworkers have provided[32] a high resolution XPS study of the core- and valence-level spectra of amorphous SiO_2 films (thermally grown on silicon substrate) as well as the Si/SiO_2 interface. Employing newly developed spectral reconstruction procedures, these authors have demonstrated the presence of two dominant and one weak discreet peak structure in the Si(2*p*) envelope in amorphous SiO_2 (Fig. 9). The central peak, shifted by 4.5 eV from the silicon substrate 2*p* value, has been identified as corresponding to the expected predominance of six-membered rings of α-quartz. Thus utilizing our calculated charge loss of 2.04 (parameters of set 2) from a central silicon to four oxygens for a Si-O-Si bridging bond angle of 144°, we obtain the value 2.20 for the Si (2*p*) scale factor, η_{Si}. Use of this scale factor places the lower and higher observed Si(2*p*) peaks in Fig. 9 at Si-O-Si bond angles in the neighborhood of 170° and 125°, respectively. For the purpose of charge transfer we have employed parameters of set 2 since this set attempts to fit all the bands, conduction and valence, whereas set 4 is a fit to the valence bands alone. Consequently, set 2 has a more stringent requirement imposed on it. If the correlation between the Si-O-Si bond angle and ring size noted earlier can be relied upon, then the three peaks of Fig. 9 suggest the occurrence of four-membered rings (found in the polymorph coesite with angle 120°), six-membered rings (of α-quartz), and higher membered rings which may correspond to the seven- and eight-membered rings of the β-cristobalite. Thus a possible picture of amorphous SiO_2 that emerges from this analysis is one of a distribution of the bridging Si-O-Si bond angles with peaks at angles of order 120°, 144°, and 165° or higher.

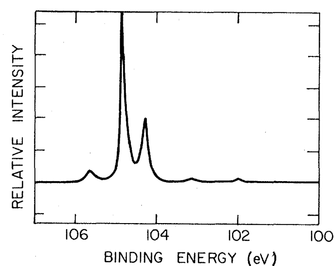

FIG. 9. Shows the deconvolved Si (2*p*) spectra for 49 Å thick oxide (from Ref. 32). For clarity the silicon substrate peak (which occurs at 4.5 eV lower binding energy than the most intense oxide peak shown) is not shown.

VI. DISCUSSION AND CONCLUSIONS

A tight-binding study of the electronic structure of α-quartz has been presented. The tight-binding parameters of α-quartz were determined by fitting to the electronic structure provided by pseudopotential-based calculations. It was found that no one set of parameters can reproduce all the desired features at once. Consequently, we have provided two sets of parameters for each of two different approximations. Most parameters were *a priori* estimated by physical considerations and the known behavior of other relevant materials. The final fitted parameters are mostly close to these estimates. Some exceptions are an unduly large separation between the diagonal energies required to reproduce the rather large band gap (~9 eV) of SiO_2, and a large $V_{p\sigma\sigma}^{Si-O}$, which, via a second-order Si-O interaction, allows the existence of an indirect gap.

It is important to note the origin of the indirect nature of the band gap since many other investigators have found a change from direct to indirect nature as a function of such parameters as the exchange parameter α. Although in principle the value of the exchange parameter α should be fixed, nevertheless, calculations employing several values of α between 0.67 and 1.0 have been reported in the literature. For instance, while Chelikowsky and Schlüter in their recent psuedopotential-based calculations[14] took $\alpha = 0.8$ and found an indirect gap $\{M(24) \rightarrow \Gamma(25)\}$, Calaberese and Fowler employing a mixed basis method took $\alpha = 1.0$ and found[33] a direct gap of 6.3 eV at Γ. For $\alpha = 0.67$ Batra has reported[34] an indirect gap of 7.6 eV, although it is at $K(24) \rightarrow \Gamma(25)$. Increasing α to 0.8, Batra finds[34] the indirect gap to remain at $K(24) \rightarrow \Gamma(25)$, although its magnitude is enhanced to 8.7 eV. Furthermore, within the parametrized tight-binding procedure such as ours, but fitting to certain experimental data, Chadi *et al.* found[35] the indirect gap to be at $A(24) \rightarrow \Gamma(25)$. These authors also found β-cristobalite to have a smaller and direct gap at Γ of 6.9 eV. The trend towards a smaller gap for a Si-O-Si bond angle of 180° is opposite to that found by Batra, by Calaberese and Fowler, and by us. This wide quantitative—as well as qualitative—spread in the reported results for the electronic structure of SiO_2 makes the exposition of the role and interplay of various parameters in a tight-binding study of paramount importance. The subtle interplay of second-order effects controlling the direct-indirect nature, its positioning (M to Γ or K to Γ or otherwise) and magnitude of the fundamental band gap as exposed in our study, thus take on a particular significance.

The topmost valence bands are found to be derived from the nonbonding oxygen $2p$ orbitals. Thus the parameter controlling these bands, particularly their dispersion, is the oxygen-oxygen nearest-neighbor interactions, although the Si-O nearest-neighbor interactions do influence these bands in higher orders of the interaction. This introduces a certain amount of bonding character to these bands as well, although it is very small. Furthermore, in Sec. III we showed that the major influence of the oxygen-oxygen interactions arises from the separation of these atoms in the structure, rather than the Si-O-Si bond angle. This tends to substantiate the inference drawn by Fischer *et al.* from their work[15] on $Si_xGe_{1-x}O_2$.

Results for the density of states (DOS) were presented for α-quartz, showing their s and p character. This again indicates the small contribution of s states to the valence bands near the fundamental band gap. A substantial dip in the DOS in the energy region between the bonding and nonbonding valence bands is found. The s and p partial DOS were weighted by the appropriate photoelectric cross sections and the resulting total weighted DOS is compared with the results of the recent XPS determinations for crystalline α-quartz, as well as amorphous SiO_2. The main features are well reproduced, the major deficiency being too high a peak at the leading edge of the nonbonding valence bands near the band gap. This is caused by a lack of sufficient dispersion in the nonbonding bands. This is a carryover from the psuedopotential calculations which also give rise to very narrow nonbonding bands. We can remove the deficiency easily by determining some of the tight-binding parameters via a fit to certain experimentally determined values. However, in this study we decided not to mix theoretical and experimental values in determining the values of the fitted parameters. This maintains a certain consistency in the study, as well as avoids additional ambiguities and uncertainties in the interpretation of the results arising from variations in the parameters. Finally, the charge transfer to oxygen was calculated employing special points in the Brillouin zone and found to be of the order of unity.

The similarity of the optical properties of crystalline and amorphous SiO_2 suggest that only short-range order may be the dominant factor in determining the electronic structure of SiO_2. Motivated by this, we studied the influence of short-range distortions by varying the flexible Si-O-Si bridging bond angle θ, the oxygen-oxygen separation, as well as the more rigid tetrahedral angle at Si. We found that a Si-O-Si bond angle smaller than 144° gives rise to a filling of the dip (via a decrease in $V_{p\sigma\sigma}^{Si-O}$) in the density of states between the bonding and nonbonding bands, but at the same time tends to increase the fundamental band gap predominant-

ly by lowering the valence band edge. The opposite behavior is found for Si-O-Si bond angles larger than 144°. The true behavior of the amorphous phase is undoubtedly some statistically averaged behavior arising from a distribution of these bond angles.

Experiments on amorphous SiO_2 films reveal a smaller fundamental band gap, as well as filling of the dip in the DOS in the region between bonding and nonbonding valence bands, thus indicating a definite presence of larger as well as smaller Si-O-Si bond angles.

In an effort to shed some light on this fundamental matter of the distribution of the Si-O-Si bond angles, we took the first step towards correlating local structure variations and the chemical shifts of the core levels. A conceptual framework relating the variations in the valence charge distribution induced by structural distortions to the shift in the core-level binding energies was presented. Analysis of the existing data on this basis reveals that the distribution of the Si-O-Si bond angle does indeed show predominance of certain bond angles, which are likely to be in the neighborhood of 120°, 144°, and 165°. Correlating these angles with the known angles in various polymorphs of SiO_2, we note that the above-mentioned distribution of bridging oxygen bond angle may be a reflection of a more fundamental aspect of the structure of amorphous SiO_2 (and possible nonmetallic glassy materials in general), namely, a distribution of the size of rings formed of SiO_4 tetrahedron. A realistic consideration of the stability of a ring of a given size in the amorphous phase is not within the present reach of our understanding of glass materials, although some consideration of the stability of isolated rings (and some inference regarding glassy materials) was started a few decades ago.[26,27]

ACKNOWLEDGMENTS

This work was supported in part by ONR Contract No. 00014-77-C-0397. One of us (A.M.) is grateful to the A.P. Sloan Foundation for a fellowship which has partially supported this work.

[1]A brief summary of a substantial part of this work was presented at the International Conference on *Physics of SiO_2 and Its Interfaces*, edited by S. T. Pantelides, (Pergamon, New York, 1978), p. 60.

[2]A. F. Ruffa, Phys. Status Solidi 29, 605 (1968).

[3]M. H. Reilly, J. Phys. Chem. Solids 31, 1041 (1970).

[4]I. V. Abarenkov, A. V. Amosov, V. F. Bratsev, and D. M. Yudin, Phys. Status Solidi 2, 865 (1970).

[5]A. F. Ruffa, J. Non-Cryst. Solids 13, 37 (1973/74).

[6]A. J. Bennett and L. M. Roth, J. Phys. Chem. Solids 32, 1251 (1971); Phys. Rev. B 4, 2686 (1971).

[7]G. A. D. Collins, D. W. J. Cruickshank, and A. Breeze, J. Chem. Soc. Faraday Trans. II 68, 1189 (1972).

[8]T. L. Gilbert, W. J. Stevens, H. Schrenk, M. Yoshimine, and P. S. Bagus, Phys. Rev. B 8, 5988 (1973).

[9]T. A. Tossell, D. J. Vaughan, and K. H. Johnson, Chem. Phys. Lett. 20, 329 (1973).

[10]K. L. Yip and W. B. Fowler, Phys. Rev. B 10, 1400 (1974).

[11]P. M. Schneider and W. B. Fowler, Phys. Rev. Lett. 36, 425 (1976).

[12]S. T. Pantelides and W. A. Harrison, Phys. Rev. B 13, 2667 (1976).

[13]S. Ciraci and I. P. Batra, Phys. Rev. B 15, 4923 (1977).

[14]J. R. Chelikowsky and H. Schluter, Phys. Rev. B 15, 4020 (1977).

[15]B. Fischer, R. A. Pollak, T. H. DiStefano, and W. D. Grobman, Phys. Rev. B 15, 3193 (1977).

[16]F. J. Grunthaner and J. Maserjian, in *Physics of SiO_2 and its Interfaces*, edited by S. T. Pantelides (Pergamon, New York, 1978), p. 389.

[17]H. Jones, *Theory of Brillouin Zones and Electronic States in Crystals* (North-Holland/Elsevier, Amsterdam, 1975).

[18]R. W. G. Wyckoff, *Crystal Structures*, 2nd ed. (Interscience, New York, 1963), Vol. I, p. 312.

[19]J. C. Slater and G. F. Koster, Phys. Rev. 94, 1948 (1954).

[20]D. J. Chadi and M. L. Cohen, Phys. Rev. B 8, 5747 (1973).

[21]K. C. Pandey and J. C. Phillips, Phys. Rev. B 13, 750 (1976).

[22]J. H. Scofield, J. Electron Spectrosc. Relat. Phenom. 8, 129 (1976).

[23]See, for example, A. G. Revesz, J. Non-Cryst. Solids, 7, 77 (1972) and references therein.

[24]R. N. Nucho and P. A. Wolff (unpublished).

[25]K. Siegbahn *et al.* in *ESCA: Atomic, Molecular and Solid State Structure Studied by Means of Electron Spectroscopy* (Almqvist and Wiksells, Uppsala, 1967).

[26]W. H. Zachariasen, Z. Krist. 54, 3841 (1932).

[27]T. Zoltai and M. J. Buerger, Z. Kristalla, 114, 1 (1960).

[28]R. J. Bell and P. Dean, Philos. Mag. 25, 1381 (1972).

[29]K. Hubner, Phys. Status Solidi A 40, 133 (1977), 40, 487 (1977), 42, 501 (1977); K. Hubner and A. Lehmann, Phys. Status Solidi A 46, 451 (1978).

[30]R. C. Gray, J. C. Carver, and D. M. Hercules, J. Electron. Spectrosc. Relat. Phenom. 8, 343 (1976).

[31]Recently Hubner (Ref. 29) has revised his ionicity verus Si-O-Si bond angle curve, suggesting a bell-shaped curve rather than a monotonically increasing one. An examination of Hubner's analysis shows that a 4% uncertainty in the experimental value of $\epsilon_1(0)$, used for α-quartz, for instance, leads to approximately 6% uncertainty in the corresponding value of the ionicity. In the range of ionicities examined (0.52–0.64), this 6% uncertainty amounts to one quarter of the entire range. Uncertainties of the order of 2–5% in experimental values of $\epsilon_1(0)$ being quite common, it follows that the

bell-shaped curve of Ref. 29 cannot be relied upon.

[32]F. J. Grunthaner, P. J. Grunthaner, R. P. Vasquez, B. F. Lewis, J. Maserjian, and A. Madhukar, J. Vac. Sci. Technol. (to be published).

[33]E. Calaberese and W. Beall Fowler, Phys. Rev. B 18, 2888 (1978).

[34]I. Batra, in *Physics of SiO_2 and Its Interfaces*, edited by S. T. Pantelides (Pergamon, New York, 1978), p. 65 .

[35]D. J. Chadi, R. B. Laughlin, and J. K. Joannopoulos, in *Physics of SiO_2 and Its Interfaces*, edited by S. T. Pantelides (Pergamon, New York, 1978) p. 55.